R9AP targeting to rod outer segments is independent of rhodopsin and is guided by the SNARE homology domain

Jillian N. Pearring[a], Eric C. Lieu[a], Joan R. Winter[a], Sheila A. Baker[b], and Vadim Y. Arshavsky[a]
[a]Albert Eye Research Institute, Duke Eye Center, Duke University, Durham, NC 27710; [b]Department of Biochemistry and Ophthalmology and Visual Sciences, Carver College of Medicine, University of Iowa, Iowa City, IA 52242

ABSTRACT **In vertebrate photoreceptor cells, rapid recovery from light excitation is dependent on the RGS9·Gβ5 GTPase-activating complex located in the light-sensitive outer segment organelle. RGS9·Gβ5 is tethered to the outer segment membranes by its membrane anchor, R9AP. Recent studies indicated that RGS9·Gβ5 possesses targeting information that excludes it from the outer segment and that this information is overridden by association with R9AP, which allows outer segment targeting of the entire complex. It was also proposed that R9AP itself does not contain specific targeting information and instead is delivered to the outer segment in the same post-Golgi vesicles as rhodopsin, because they are the most abundant transport vesicles in photoreceptor cells. In this study, we revisited this concept by analyzing R9AP targeting in rods of wild-type and rhodopsin-knockout mice. We found that the R9AP targeting mechanism does not require the presence of rhodopsin and further demonstrated that R9AP is actively targeted in rods by its SNARE homology domain.**

Monitoring Editor
Patrick J. Brennwald
University of North Carolina

Received: Feb 18, 2014
Revised: Jun 5, 2014
Accepted: Jul 1, 2014

INTRODUCTION

Photoreceptors are highly polarized neurons with all molecular components involved in generating a light response confined to the ciliary outer segment organelle. Because the outer segment exists in a state of constant renewal, its resident proteins are continuously transported into this compartment. Accordingly, photoreceptors serve as a productive model for studying ciliary protein targeting, sorting, and trafficking.

One interesting consequence of ongoing outer segment renewal is that it requires a very significant flux of transport vesicles delivering newly synthesized proteins and lipids to this compartment. A by-product of this phenomenon is that membrane proteins lacking specific intracellular targeting information tend to accumulate in the outer segment. This "default pathway" for untargeted protein trafficking is particularly striking in frog rods, which contain very large outer segments. It was first noted by Papermaster and colleagues (Tam *et al.*, 2000; Moritz *et al.*, 2001), who demonstrated that only a small portion of a rhodopsin mutant stripped of its outer segment–targeting motif is actually mislocalized from rod outer segments. To explain this pattern, they proposed that the majority of the mutant is carried after being passively incorporated into abundant rhodopsin transport vesicles. Also using transgenic *Xenopus*, previous studies from our laboratory demonstrated that a number of other lipidated and integral membrane proteins lacking specific targeting information follow this default localization pattern (Baker *et al.*, 2008). Furthermore, deleting targeting sequences from proteins normally residing in other parts of the photoreceptor cell resulted in their predominantly outer segment localization (Baker *et al.*, 2008; Gospe *et al.*, 2010).

R9AP is a single-pass transmembrane protein that anchors the RGS9·Gβ5 GTPase- activating complex to outer segment disk membranes (Hu and Wensel, 2002). Along with tethering RGS9·Gβ5 to disk membranes, R9AP protects RGS9·Gβ5 from intracellular proteolysis and ensures RGS9·Gβ5 delivery to outer segments (reviewed in Arshavsky and Wensel, 2013). In photoreceptors, the majority of R9AP is localized to the outer segment, with a minor fraction present in the plasma membrane enclosing the rest of the cell, mostly in

This article was published online ahead of print in MBoC in Press (http://www.molbiolcell.org/cgi/doi/10.1091/mbc.E14-02-0747) on July 9, 2014.
Address correspondence to: Vadim Arshavsky (vadim.arshavsky@duke.edu).
Abbreviations used: R9AP, RGS9-1 anchor protein; RGS, regulator of G-protein signaling; SNARE, soluble *N*-ethylmaleimide–sensitive factor attachment protein receptor.

the synaptic region (Cowan *et al.*, 1998; Hu and Wensel, 2002; Martemyanov *et al.*, 2003; Song *et al.*, 2007; Baker *et al.*, 2008). In *Xenopus* rods, this peculiar expression pattern is essentially indistinguishable from the default distribution for untargeted membrane protein constructs (Baker *et al.*, 2008), which raised the hypothesis that R9AP is delivered to its intracellular destinations via the default pathway.

However, we recently showed that the predominant outer segment delivery of untargeted membrane proteins takes place only in those photoreceptors whose outer segments are very large, such as *Xenopus* rods receiving ~700 newly synthesized rhodopsin molecules each second (reviewed in Pearring *et al.*, 2013). Untargeted proteins expressed in photoreceptors containing smaller outer segments, such as mouse rods, display a more balanced distribution between the outer segment and the rest of the cell. In this case, the intracellular localization of R9AP, still prominent in outer segments, is distinctly different from that of untargeted membrane proteins (Pearring *et al.*, 2013). This suggested that, at least in mouse rods, R9AP is actively targeted to its intracellular destinations. We now report that the outer segment targeting of R9AP in the mouse is indeed completely independent of rhodopsin and that R9AP contains a specific targeting region confined within its *N*-ethylmaleimide–sensitive factor (SNARE) homology domain.

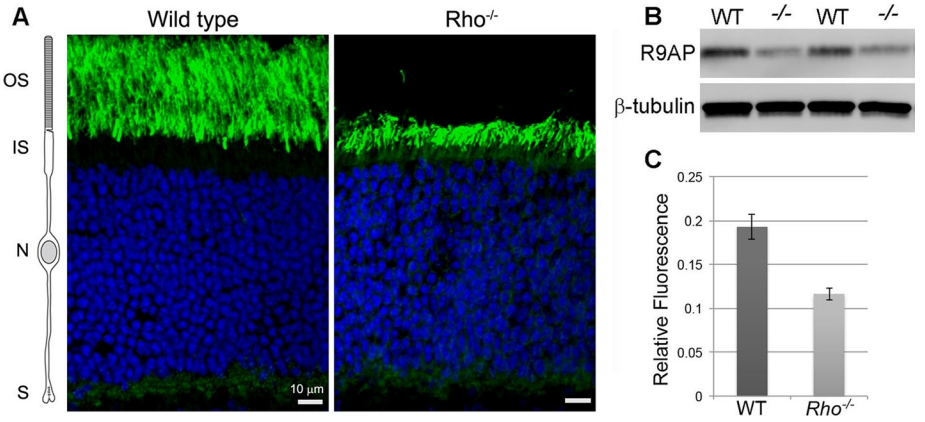

FIGURE 1: R9AP localization and expression in rhodopsin-knockout mice. (A) R9AP (green) immunostaining of retinal cross sections from *Rho*$^{-/-}$ and wild-type mice (bars, 10 µm). Nuclei are counterstained with Hoechst (blue). (B) Representative Western blot showing R9AP and β-tubulin bands in wild-type (WT) and *Rho*$^{-/-}$ (-/-) retinas. (C) The signal intensity of each R9AP Western blot band was normalized to the density of the β-tubulin band and plotted as a relative fluorescence. The data are averaged from measurements performed with six wild-type and six *Rho*$^{-/-}$ retinal samples.

RESULTS

R9AP is targeted to the outer segment in the absence of rhodopsin

The most straightforward approach to determining whether R9AP has its own outer segment–targeting information or is passively incorporated into abundant rhodopsin transport vesicles is to analyze R9AP localization in rods of rhodopsin-knockout (*Rho*$^{-/-}$) mice. Although normal rod outer segments are not formed in these animals, eventually leading to photoreceptor degeneration, rods of young *Rho*$^{-/-}$ mice develop small membrane extensions emerging from the distal connecting cilium (Humphries *et al.*, 1997; Lem *et al.*, 1999; Lee *et al.*, 2006). A previous study found that another outer segment–specific protein, peripherin, is reliably targeted to these "rudimentary outer segments," which argues that peripherin is trafficked independently of rhodopsin (Lee *et al.*, 2006). We tested whether the same is true for R9AP.

R9AP immunostaining in retinal cross sections of *Rho*$^{-/-}$ mice was performed on postnatal day 21, when the rudimentary outer segments are fully formed but photoreceptor degeneration has not yet begun (Figure 1A). Despite a dramatic reduction in the outer segment volume in these animals, *Rho*$^{-/-}$ retinas contain ~60% of normal R9AP content (Figure 1, B and C). Remarkably, nearly all R9AP in these retinas is still found in the rudimentary outer segments, and the less prominent synaptic immunostaining is preserved as well. This localization pattern is consistent with that in wild-type retinas, apart from the size and shape of the outer segments (Figure 1A). These results establish the independence of R9AP outer segment trafficking from that of rhodopsin and suggest that R9AP contains specific targeting information encoded in its sequence. This hypothesis was tested in the next set of experiments.

The targeting of R9AP in mouse rods requires its SNARE homology domain

A series of FLAG-tagged R9AP fragments representing various combinations of its constituent domains was placed downstream of a rod-specific rhodopsin promoter and introduced into wild-type mouse retinas by in vivo electroporation (Matsuda and Cepko, 2004). R9AP contains three principal domains, as illustrated in Figure 2A: the N-terminal Habc putative trihelical bundle, the SNARE homology domain, and the C-terminal transmembrane domain. We first established the baseline R9AP distribution in mouse rods by analyzing the localization of a FLAG-tagged full-length R9AP. Individual cells that were successfully transfected exhibited prominent FLAG staining in the outer segment, with a small fraction also detected in the rod synaptic terminal, essentially replicating the localization pattern of endogenous R9AP protein (Figure 2B).

The absence of the Habc domain did not cause a notable change in this localization pattern (Figure 2C). The same was observed upon deletion of both Habc domain and the linker between Habc and SNARE homology domains (Figure 2D). However, the deletion of the SNARE homology domain redirected a large portion of the expressed protein to other cellular compartments (Figure 2E). A hallmark of this mislocalization is the appearance of stained plasma membrane contours around the nuclei of transfected rods. A similar mislocalization pattern was observed for the construct consisting of the transmembrane domain alone (Figure 2F).

We then compared the distribution of these mislocalized R9AP fragments with that of an untargeted membrane construct, the first transmembrane domain of the mGluR1 receptor fused to green fluorescent protein (GFP; Baker *et al.*, 2008). The overall localization pattern for this untargeted construct mirrored that of both mislocalized R9AP fragments (Figure 2G; see also Pearring *et al.* [2013] for another example of a GFP-fused transmembrane domain from the activin receptor).

Formal quantification analysis described in *Materials and Methods* revealed no statistical significance among the distributions of FLAG-tagged R9AP and the two constructs retaining the SNARE homology domain. The outer segment fraction of R9AP was calculated as 82 ± 8%, whereas FLAG-R9APΔHabc was 75 ± 7%

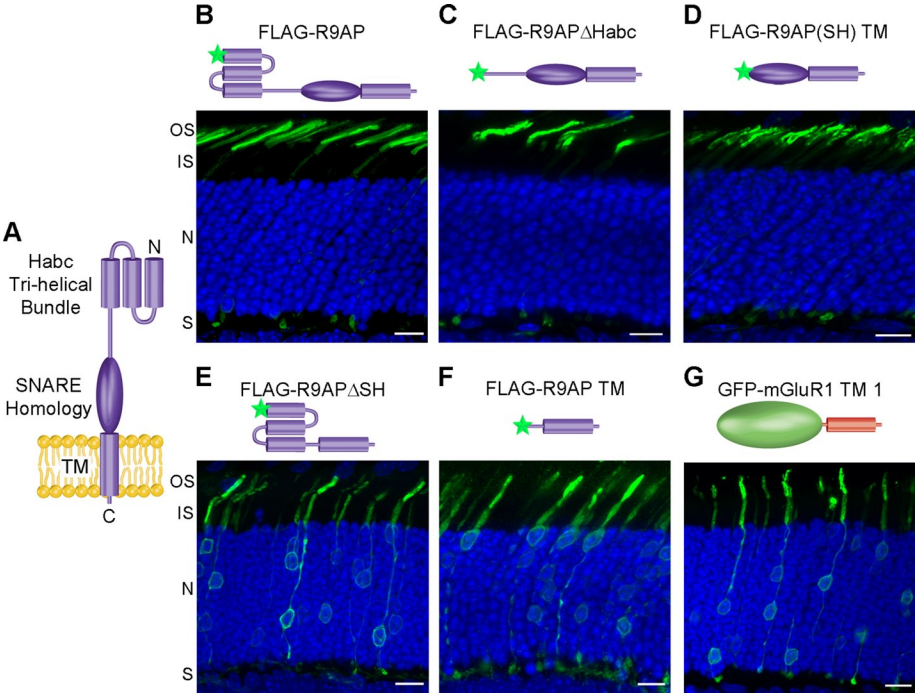

FIGURE 2: Localization of FLAG-tagged R9AP constructs in mouse rods. (A) Cartoon diagram illustrating R9AP domain composition: Habc trihelical bundle, SNARE homology, and transmembrane (TM). The following FLAG-tagged constructs were electroporated into wild-type mouse rods: (B) full-length R9AP, (C) R9AP lacking Habc, (D) SNARE homology (SH) fused to transmembrane domain, (E) Habc fused to transmembrane domain, (F) transmembrane domain alone, and (G) GFP-tagged transmembrane segment 1 from mGluR1. Nuclei are counterstained with Hoechst (blue). IS, inner segment; OS, outer segment; N, outer nuclear layer; S, synapses. Bars, 10 µm. Each construct is illustrated schematically at the top, with the FLAG tag depicted as a green star.

($p = 0.34$), and FLAG-R9AP(SH)-TM was 76 ±4 % ($p = 0.22$). In contrast, the difference between distributions of these constructs and those lacking the SNARE homology domain reached high statistical significance, with $p < 0.004$ in all cases. When the distributions of two constructs lacking the SNARE homology domain (34 ± 5% in outer segments for both FLAG-R9APΔSH and FLAG-R9AP-TM) was compared with that of an untargeted construct (41 ± 10%), no statistically significant difference was observed ($p > 0.25$), consistent with the lack of active targeting.

Taken together, our results suggest that R9AP's intracellular targeting information is encoded within the SNARE homology domain.

SNARE homology domain is sufficient for normal R9AP targeting

In the next experiment, we tested whether R9AP's SNARE homology domain is sufficient to achieve normal R9AP localization in rods. This required expressing this domain without its adjacent transmembrane domain serving as a means of R9AP membrane attachment. In a previous study, we showed that replacing the transmembrane domain of full-length R9AP with a C-terminal CCaaX box (CCIIL) for double lipidation (palmitoylation and geranylgeranylation) preserves both normal R9AP intracellular localization and normal RGS9·Gβ5 binding (Gospe *et al.*, 2011). Therefore we expressed a construct containing the SNARE homology domain of R9AP directly fused to the CCIIL sequence. This construct displayed a distribution pattern indistinguishable from that of full-length R9AP (compare Figure 3A with Figure 2B), suggesting that the SNARE homology domain is sufficient for normal R9AP targeting. In two control experiments, we demonstrated that constructs containing the CCIIL sequence at the C-termini of either the Habc domain of R9AP or GFP followed an untargeted distribution pattern observed for the corresponding transmembrane constructs (compare Figure 3, B and C, with Figure 2, E and G). Repeating the quantification for lipidated constructs revealed statistically significant difference ($p = 0.00002$) in the distributions of FLAG-R9AP(SH)-CCIIL (90 ± 5% in outer segments) and GFP-CCIIL (38 ± 3%) and lack thereof ($p = 0.1$) between FLAG-R9AP(Habc)-CCIIL (42 ± 3%) and GFP-CCIIL.

Previous studies suggested that R9AP is the only protein in photoreceptors that has a SNARE homology domain and is expressed almost exclusively in the outer segment (Kwok *et al.*, 2008; Skiba *et al.*, 2013). We illustrated this point in an additional set of experiments in which we compared the intracellular targeting of the R9AP SNARE homology domain with two other SNARE domains. A previous study in *Xenopus* rods showed that the SNARE domain of syntaxin 3 is responsible for its normal targeting to the portions of the plasma membrane enclosing the inner segment and synaptic terminal (Baker *et al.*, 2008). To determine whether the same was true in mouse rods, we electroporated wild-type mouse retinas with a membrane-anchored construct encoding the SNARE domain of syntaxin 3 (Figure 4A). This construct was actively excluded from the outer segment, following the localization pattern described for full-length syntaxin 3 in frogs and mice (Chuang *et al.*, 2007; Baker *et al.*, 2008; Mazelova *et al.*, 2009). However, when we expressed the SNARE homology domain of R7BP, an R9AP homologue not endogenous to photoreceptors (Martemyanov *et al.*, 2005; Cao *et al.*, 2010), it was distributed throughout all compartments of the rod cell, behaving as an untargeted membrane protein (Figure 4B). Both distribution patterns are in striking contrast to the SNARE homology domain from R9AP (Figures 4C and 2D), highlighting the

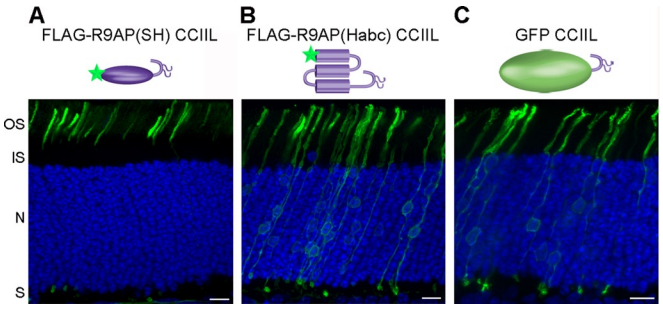

FIGURE 3: The SNARE homology domain is sufficient for normal R9AP targeting. Representative images of wild-type mouse retinas electroporated with the following CCIIL fused constructs: (A) FLAG-tagged SNARE homology (SH) domain, (B) FLAG-tagged Habc domain, and (C) GFP. Bars, 10 µm.

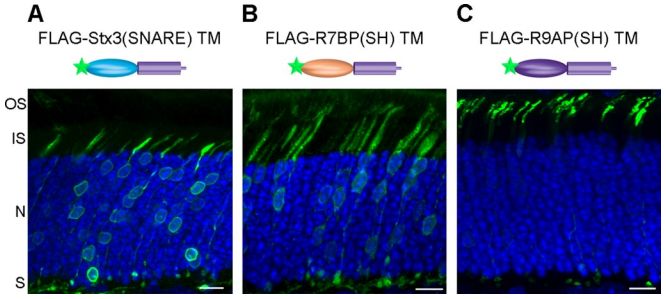

FIGURE 4: Subcellular localization of various SNARE homology domains expressed in mouse rods. Wild-type mouse retinas were electroporated with three FLAG-tagged SNARE homology domains fused to the transmembrane domain of R9AP: (A) syntaxin 3, (B) R7BP, and (C) R9AP. Bars, 10 µm.

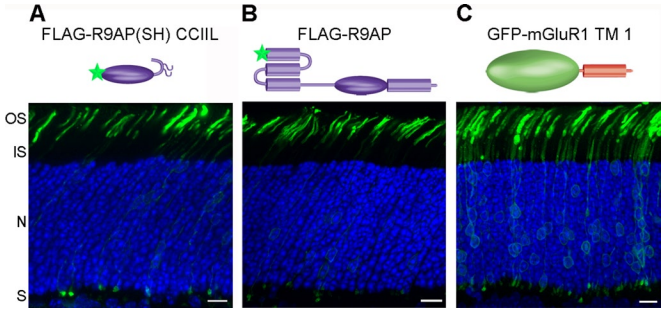

FIGURE 5: Intracellular targeting of R9AP's SNARE homology domain is independent of endogenous R9AP. Images of *R9AP*$^{-/-}$ mouse retinas electroporated with the following constructs: (A) CCIIL fused, FLAG-tagged SNARE homology domain, (B) FLAG-tagged full-length R9AP, and (C) GFP-tagged transmembrane segment 1 from mGluR1. Bars, 10 µm.

versatility of SNARE domains in guiding photoreceptor protein targeting.

Intracellular targeting of R9AP SNARE homology domain is independent of endogenous R9AP

The notion that R9AP's targeting information is localized within its SNARE homology domain is based on the assumption that recombinant constructs containing this domain do not form oligomeric complexes (with other SNARE proteins or the endogenous R9AP), as other SNARE domains typically do (Rizo and Sudhof, 2012). Previous studies revealed R9AP is not bound to other SNARE proteins in the outer segment disk membranes (Hu and Wensel, 2002), and the R9AP content in these membranes is significantly larger than that of any other SNARE protein (Kwok *et al.*, 2008; Skiba *et al.*, 2013), precluding a possibility for stoichiometric complex formation. However, the possibility of R9AP homo-oligomerization, although not reported, had not been ruled out.

We therefore expressed the lipidated SNARE homology domain of R9AP in rods of R9AP-knockout (*R9AP*$^{-/-}$) mice. *R9AP*$^{-/-}$ rods are morphologically normal but do not contain endogenous R9AP or its cognate RGS9 and Gβ5 partners (Keresztes *et al.*, 2004). The data in Figure 5A show that the intracellular distribution of the R9AP SNARE homology domain in *R9AP*$^{-/-}$ rods is indistinguishable from that in normal rods, thereby establishing that the targeting of this construct does not rely on oligomerization with endogenous R9AP. A positive control illustrates normal targeting of the full-length R9AP construct in *R9AP*$^{-/-}$ rods (Figure 5B), whereas a negative control shows the distribution of an untargeted membrane construct for comparison (Figure 5C). These data solidify our conclusion that the SNARE homology domain is both necessary and sufficient to determine the subcellular localization of R9AP in photoreceptors.

DISCUSSION

In all cells, membrane proteins are sorted in the endoplasmic reticulum and *trans*-Golgi network, where they are packaged into vesicles for transport to their intracellular destinations. Photoreceptor cells are defined by their highly active trafficking pathway in which proteins synthesized and processed in the inner segment are delivered to the outer segment undergoing continuous renewal. The importance of outer segment protein trafficking is highlighted by observations that some of the most severe cases of inherited retinal degeneration are caused by mutations that affect this trafficking flow (Bessant *et al.*, 1999; Berson *et al.*, 2002; Berger *et al.*, 2010). Although significant progress has been made in understanding rhodopsin trafficking (Sung and Chuang, 2010; Pearring *et al.*, 2013; Wang and Deretic, 2014), many critical aspects of this pathway remain unknown, and even less is known about targeting and trafficking of other outer segment–resident proteins.

One of the most challenging hurdles to studying protein trafficking has been the identification of targeting signals in the protein sequence. Among all proteins residing exclusively in the outer segment (Skiba *et al.*, 2013), distinct outer segment–targeting sequences have been identified only for rhodopsin, peripherin, and retinal dehydrogenase (Sung *et al.*, 1994; Deretic *et al.*, 1998; Tam *et al.*, 2000, 2004; Luo *et al.*, 2004; Salinas *et al.*, 2013). The identification of the SNARE homology domain as the active targeting region directing R9AP primarily to the outer segments of mouse rods is another major step in this direction. Of interest, there is no evident similarity between the sequence of the SNARE homology domain in R9AP and other outer segment targeting sequences. This directs future experiments to address whether each of these proteins is packaged into outer segment–bound vesicles using a unique set of protein–protein interactions or there is a universal protein-sorting mechanism able to interpret such apparently dissimilar targeting information. A closely related question is whether in wild-type rods R9AP is copackaged for outer segment delivery in the same vesicles as rhodopsin or an entirely unique trafficking route is used. Another interesting problem to consider, which is unique to R9AP, is to explain the targeting mechanism responsible for its dual localization pattern, being present in both the outer segment and synaptic terminal. In addition, the functional role that R9AP plays in the synaptic terminals of photoreceptor cells remains to be elucidated.

Of particular significance in the context of this study is to reconcile the conclusions on R9AP targeting in mouse and frog rods. Our findings indicate that in mouse rods, R9AP is actively targeted to its intracellular destinations using the information encoded in the SNARE homology domain. This conclusion contrasts our previous interpretation that in frog rods, R9AP uses the default trafficking pathway described in the *Introduction* (Baker *et al.*, 2008). This interpretation was driven by striking similarity between the intracellular distributions of R9AP and untargeted protein constructs expressed in frog rods, both predominant in the outer segment, with a small fraction in the plasma membrane enclosing the rest of the cell. Furthermore, the localization patterns of R9AP and its mutant lacking the SNARE homology domain are essentially identical in the frog. In contrast, untargeted membrane proteins expressed in mouse rods still access the outer segment but are also abundant throughout the inner segment membranes. In this case, the distribution of R9AP and its SNARE homology domain (Figure 2, B and D) could not be

confused with that of a randomly chosen untargeted transmembrane construct (Figure 2G) or other SNARE domains that we expressed in mouse rods (Figure 4, A and B). This difference was critical for our ability to establish the existence of active R9AP targeting in this animal model.

Our demonstration of active R9AP targeting in mouse rods also calls for a reconsideration of the mechanism of R9AP targeting in frogs. Unfortunately, the equivalence between distribution patterns of R9AP and untargeted proteins in this case deem existing experimental tools insufficient to test whether frog R9AP follows default intracellular distribution or uses its SNARE homology domain for active targeting. This could change, however, if a frog model with skewed default trafficking pattern (e.g., rhodopsin knockout) becomes available in the future. Meanwhile, further studies of the R9AP targeting mechanism can use the mouse as a primary model.

MATERIALS AND METHODS

Antibodies and mouse strains

Rabbit antibody against R9AP sequence 144–223 is described in Keresztes *et al.* (2003). Anti-GFP antibody conjugated to Alex 488 was obtained from Invitrogen (Grand Island, NY), monoclonal mouse anti-FLAG M2 antibody from Sigma-Aldrich (St. Louis, MO), and anti-β-tubulin D66 antibody from Abcam (Cambridge, MA). The *R9AP*$^{-/-}$ mouse is described in Keresztes *et al.* (2004) and the *Rho*$^{-/-}$ mouse in Lem *et al.* (1999). CD-1 wild-type mice (Charles River, Moorisville, NC) were used in electroporation experiments, whereas C57BL/6J wild-type mice (Jackson Labs, Bar Harbor, ME) were used for immunofluorescence and Western blotting.

In vivo electroporation of mouse retinas

DNA constructs were electroporated into the retinas of neonatal mice (Matsuda and Cepko, 2004), using a detailed protocol from Gospe *et al.* (2011). The plasmid driving gene expression under the pRho promoter (Matsuda and Cepko, 2004) was obtained from Addgene (Cambridge, MA; plasmid 11156). All DNA constructs were cloned between *Age*I and *Not*I sites in pRho. The FLAG-tagged mouse R9AP (Gospe *et al.*, 2011) construct was used as a template for generating mutant constructs by PCR. The amino acid sequences for each R9AP domain were defined as follows: Habc, 1–114; linker, 115–152; SNARE homology, 153–202; transmembrane, 203–238. The SNARE domain from syntaxin 3 (residues 200–249) was amplified by PCR from mouse retinal cDNA. The SNARE homology domain of R7BP (residues 179–222) was amplified from a FLAG-tagged R7BP vector provided by Kendall Blumer (Washington University, St. Louis, MO). The GFP-tagged mGluR1 transmembrane domain 1 described in Baker *et al.* (2008) was cloned into the pRho plasmid. The CAAX-box (CCIIL) sequence was directly attached to the C-terminal of R9AP's SNARE homology and R9AP's Habc domain or GFP, which included a seven–amino acid upstream linker (ACDPSKA), using overlapping primers. Primers introducing 5′ *Age*I sites and 3′ *Not*I sites were designed for each construct and are available upon request. At least four animals yielding consistent results were analyzed for each construct.

Immunofluorescence

Immunostaining of the endogenous R9AP was performed using OCT-embedded frozen retina sections (Hu and Wensel, 2002; Cao *et al.*, 2009; Jeffrey *et al.*, 2010). As described in these publications, the sections were fixed in 4% paraformaldehyde for only 15 min, which is critical to observe R9AP staining in photoreceptor synapses.

Immunostaining of electroporated constructs was performed using agarose-embedded retina sections as previously described with minor modifications (Salinas *et al.*, 2013). Briefly, posterior eyecups from mouse eyes were fixed in 4% paraformaldehyde for 1 h, rinsed in phosphate-buffered saline, and embedded in 7% low-melt agarose (Sigma-Aldrich). Vibratome cross sections of 100 µm were collected in 24-well plates, blocked in 5% goat serum in the presence of 0.5% Triton X-100, incubated overnight with the appropriate primary antibody diluted in blocker, and stained with the corresponding secondary antibody and 10 mg/ml Hoechst 33342 (Invitrogen) to label nuclei. Stained sections were coverslipped using Immu-Mount (Thermo Scientific, Waltham, MA) and visualized using a Nikon Eclipse 90i microscope and a C1 confocal scanner controlled by EZ-C1, version 3.10 software (Nikon, Melville, NY). Manipulation of images was limited to adjusting the brightness level, image size, and cropping using either EZ-C1, version 3.10, Viewer or Photoshop (Adobe, San Jose, CA).

To determine whether the subcellular distribution of each electroporated construct differs from that of untargeted membrane constructs, we performed a standard *t* test after calculating their fluorescence intensity in rod outer segments and cell bodies using the ImageJ software in the following sequence. The borders of outer segments and photoreceptor somas (including both inner segment and nuclear region) were mapped across the entire retina section. Fluorescence intensities for each area were calculated by ImageJ. The background fluorescence in each image was determined by averaging the signal intensity outside the photoreceptor layer where no expression of tagged proteins is possible, recalculated for the areas represented by outer segments and cell bodies, and subtracted from the corresponding fluorescence values. A minimum of four sections from individual mice were analyzed for each construct.

Western blot analysis

Western blotting was performed as in Gospe *et al.* (2011), using the Odyssey imaging system (LiCor, Lincoln, NE) for band visualization and quantification. Total protein concentration was measured using the RC DC Protein Assay kit (Bio-Rad, Hercules, CA). Linear ranges for R9AP and β-tubulin detection were identified in a series of sample dilutions.

ACKNOWLEDGMENTS

This work was supported by National Institutes of Health Grants EY22508 (J.N.P.), EY12859 (V.Y.A.), and EY20542 (S.A.B.), National Institutes of Health Core Grant for Vision Research EY5722, and an unrestricted grant from Research to Prevent Blindness to Duke University.

REFERENCES

Arshavsky VY, Wensel TG (2013). Timing is everything: GTPase regulation in phototransduction. Invest Ophthalmol Vis Sci 54, 7725-7733.

Baker SA, Haeri M, Yoo P, Gospe SM 3rd, Skiba NP, Knox BE, Arshavsky VY (2008). The outer segment serves as a default destination for the trafficking of membrane proteins in photoreceptors. J Cell Biol 183, 485–498.

Berger W, Kloeckener-Gruissem B, Neidhardt J (2010). The molecular basis of human retinal and vitreoretinal diseases. Prog Retin Eye Res 29, 335–375.

Berson EL, Rosner B, Weigel-DiFranco C, Dryja TP, Sandberg MA (2002). Disease progression in patients with dominant retinitis pigmentosa and rhodopsin mutations. Invest Ophthalmol Vis Sci 43, 3027–3036.

Bessant DA, Khaliq S, Hameed A, Anwar K, Payne AM, Mehdi SQ, Bhattacharya SS (1999). Severe autosomal dominant retinitis pigmentosa caused by a novel rhodopsin mutation (Ter349Glu). Hum Mutat 13, 83.

Cao Y, Kolesnikov AV, Masuho I, Kefalov VJ, Martemyanov KA (2010). Membrane anchoring subunits specify selective regulation of RGS9·Gb5 GAP complex in photoreceptor neurons. J Neurosci 30, 13784–13793.

Cao Y, Masuho I, Okawa H, Xie K, Asami J, Kammermeier PJ, Maddox DM, Furukawa T, Inoue T, Sampath AP, *et al.* (2009). Retina-specific GTPase accelerator RGS11/G beta 5S/R9AP is a constitutive heterotrimer

selectively targeted to mGluR6 in ON-bipolar neurons. J Neurosci 29, 9301–9313.
Chuang JZ, Zhao Y, Sung CH (2007). SARA-regulated vesicular targeting underlies formation of the light-sensing organelle in mammalian rods. Cell 130, 535–547.
Cowan CW, Fariss RN, Sokal I, Palczewski K, Wensel TG (1998). High expression levels in cones of RGS9, the predominant GTPase accelerating protein of rods. Proc Natl Acad Sci USA 95, 5351–5356.
Deretic D, Schmerl S, Hargrave PA, Arendt A, McDowell JH (1998). Regulation of sorting and post-Golgi trafficking of rhodopsin by its C-terminal sequence QVS(A)PA. Proc Natl Acad Sci USA 95, 10620–10625.
Gospe SM 3rd, Baker SA, Arshavsky VY (2010). Facilitative glucose transporter Glut1 is actively excluded from rod outer segments. J Cell Sci 123, 3639–3644.
Gospe SM 3rd, Baker SA, Kessler C, Brucato MF, Winter JR, Burns ME, Arshavsky VY (2011). Membrane attachment is key to protecting transducin GTPase-activating complex from intracellular proteolysis in photoreceptors. J Neurosci 31, 14660–14668.
Hu G, Wensel TG (2002). R9AP, a membrane anchor for the photoreceptor GTPase accelerating protein, RGS9-1. Proc Natl Acad Sci USA 99, 9755–9760.
Humphries MM, Rancourt D, Farrar GJ, Kenna P, Hazel M, Bush RA, Sieving PA, Sheils DM, McNally N, Creighton P, *et al.* (1997). Retinopathy induced in mice by targeted disruption of the rhodopsin gene. Nat Genet 15, 216–219.
Jeffrey BG, Morgans CW, Puthussery T, Wensel TG, Burke NS, Brown RL, Duvoisin RM (2010). R9AP stabilizes RGS11·Gb5 and accelerates the early light response of ON-bipolar cells. Vis Neurosci 27, 9–17.
Keresztes G, Martemyanov KA, Krispel CM, Mutai H, Yoo PJ, Maison SF, Burns ME, Arshavsky VY, Heller S (2004). Absence of the RGS9·Gb5 GTPase-activating complex in photoreceptors of the R9AP knockout mouse. J Biol Chem 279, 1581–1584.
Keresztes G, Mutai H, Hibino H, Hudspeth AJ, Heller S (2003). Expression patterns of the RGS9-1 anchoring protein R9AP in the chicken and mouse suggest multiple roles in the nervous system. Mol Cell Neurosci 24, 687–695.
Kwok MC, Holopainen JM, Molday LL, Foster LJ, Molday RS (2008). Proteomics of photoreceptor outer segments identifies a subset of SNARE and Rab proteins implicated in membrane vesicle trafficking and fusion. Mol Cell Proteomics 7, 1053–1066.
Lee ES, Burnside B, Flannery JG (2006). Characterization of peripherin/rds and rom-1 transport in rod photoreceptors of transgenic and knockout animals. Invest Ophthalmol Vis Sci 47, 2150–2160.
Lem J, Krasnoperova NV, Calvert PD, Kosaras B, Cameron DA, Nicolo M, Makino CL, Sidman RL (1999). Morphological, physiological, and biochemical changes in rhodopsin knockout mice. Proc Natl Acad Sci USA 96, 736–741.
Luo W, Marsh-Armstrong N, Rattner A, Nathans J (2004). An outer segment localization signal at the C-terminus of the photoreceptor-specific retinol dehydrogenase. J Neurosci 24, 2623–2632.
Martemyanov KA, Lishko PV, Calero N, Keresztes G, Sokolov M, Strissel KJ, Leskov IB, Hopp JA, Kolesnikov AV, Chen CK, *et al.* (2003). The DEP domain determines subcellular targeting of the GTPase activating protein RGS9 *in vivo*. J Neurosci 23, 10175–10181.
Martemyanov KA, Yoo PJ, Skiba NP, Arshavsky VY (2005). R7BP, a novel neuronal protein interacting with RGS proteins of the R7 family. J Biol Chem 280, 5133–5136.
Matsuda T, Cepko CL (2004). Electroporation and RNA interference in the rodent retina in vivo and in vitro. Proc Natl Acad Sci USA 101, 16–22.
Mazelova J, Ransom N, Astuto-Gribble L, Wilson MC, Deretic D (2009). Syntaxin 3 and SNAP-25 pairing, regulated by omega-3 docosahexaenoic acid, controls the delivery of rhodopsin for the biogenesis of cilia-derived sensory organelles, the rod outer segments. J Cell Sci 122, 2003–2013.
Moritz OL, Tam BM, Papermaster DS, Nakayama T (2001). A functional rhodopsin-green fluorescent protein fusion protein localizes correctly in transgenic *Xenopus* laevis retinal rods and is expressed in a time-dependent pattern. J Biol Chem 276, 28242–28251.
Pearring JN, Salinas RY, Baker SA, Arshavsky VY (2013). Protein sorting, targeting and trafficking in photoreceptor cells. Prog Retin Eye Res 36, 24–51.
Rizo J, Sudhof TC (2012). The membrane fusion enigma: SNAREs, Sec1/Munc18 proteins, and their accomplices—guilty as charged? Annu Rev Cell Dev Biol 28, 279–308.
Salinas RY, Baker SA, Gospe SM 3rd, Arshavsky VY (2013). A single valine residue plays an essential role in peripherin/rds targeting to photoreceptor outer segments. PLoS One 8, e54292.
Skiba NP, Spencer WJ, Salinas RY, Lieu EC, Thompson JW, Arshavsky VY (2013). Proteomic identification of unique photoreceptor disc components reveals the presence of PRCD, a protein linked to retinal degeneration. J Proteome Res 12, 3010–3018.
Song JH, Song H, Wensel TG, Sokolov M, Martemyanov KA (2007). Localization and differential interaction of R7 RGS proteins with their membrane anchors R7BP and R9AP in neurons of vertebrate retina. Mol Cell Neurosci 35, 311–319.
Sung CH, Chuang JZ (2010). The cell biology of vision. J Cell Biol 190, 953–963.
Sung CH, Makino C, Baylor D, Nathans J (1994). A rhodopsin gene mutation responsible for autosomal dominant retinitis pigmentosa results in a protein that is defective in localization to the photoreceptor outer segment. J Neurosci 14, 5818–5833.
Tam BM, Moritz OL, Hurd LB, Papermaster DS (2000). Identification of an outer segment targeting signal in the COOH terminus of rhodopsin using transgenic *Xenopus laevis*. J Cell Biol 151, 1369–1380.
Tam BM, Moritz OL, Papermaster DS (2004). The C-terminus of peripherin/rds participates in rod outer segment targeting and alignment of disk incisures. Mol Biol Cell 15, 2027–2037.
Wang J, Deretic D (2014). Molecular complexes that direct rhodopsin transport to primary cilia. Prog Retin Eye Res 38, 1–19.